applied sciences

MDPI

Article

Sustainable Manufacturing Decisions through the Optimization of Printing Parameters in 3D Printing

Cheng-Jung Yang * and Sin-Syuan Wu

Program in Interdisciplinary Studies, National Sun Yat-sen University, Kaohsiung 80424, Taiwan
* Correspondence: cjyang0521@mail.nsysu.edu.tw; Tel.: +886-7-5252000 (ext. 5749)

Abstract: The 3D printers integrated with fused filament fabrication (FFF) are highly valued worldwide because of their properties, which include fast proofing, compatibility with various materials, and low printing cost. The competitiveness of FFF can be enhanced by improving printing quality. However, due to the increasing sustainability issues worldwide, there is an urgent need to lower energy consumption. In this study, we focused on fan rate, printing speed, nozzle temperature, build plate temperature, and layer thickness as factors that directly impact the dimensional accuracy, carbon dioxide emissions, and printing cost of FFF printers. Several single-objective and multiobjective optimization tasks were performed using the Taguchi method and desirability approach to implement sustainable manufacturing decisions. In single-objective optimization, the inner width, outer width, material cost, and labor cost were most easily affected by the layer thickness. The outer length, carbon dioxide emissions, and electricity cost were significantly affected by the build plate temperature. In multiobjective optimization, a different set of printing parameters can be used to optimize dimensional accuracy, carbon dioxide emissions, material cost, labor cost, and electricity cost. This study helps users to obtain optimal solutions under different optimization requirements to cope with diverse manufacturing characteristics.

Keywords: 3D printer; fused filament fabrication; sustainable manufacturing; Taguchi method; desirability approach

Citation: Yang, C.-J.; Wu, S.-S. Sustainable Manufacturing Decisions through the Optimization of Printing Parameters in 3D Printing. *Appl. Sci.* **2022**, *12*, 10060. https://doi.org/10.3390/app121910060

Academic Editor: César M. A. Vasques

Received: 14 September 2022
Accepted: 4 October 2022
Published: 6 October 2022

1. Introduction

In recent years, the characteristics of additive manufacturing, such as net shape and design flexibility, have resulted in rapid growth in the manufacturing industry. Fused filament fabrication (FFF) possesses rapid prototyping [1,2], caters to different materials [3], eliminates post-processing procedures [4,5], and requires a short processing time [6,7]. Moreover, its competitiveness can be enhanced by continuously improving printing quality [8,9]. In addition, due to the increase in sustainability issues, the efforts to reduce energy consumption [10], air pollutants [11–13], and manufacturing costs [14] can result in increased adoption of sustainable manufacturing.

Dimensional accuracy is a significant factor for quality verification. In FFF printers, there is a significant correlation between printing parameters and dimensional accuracy. For instance, nozzle temperature changes can affect the homogeneity of extruded materials and cause printing size variations. Qattawi et al. [15] proposed that nozzle temperature can affect the dimensions of printed objects. For instance, when the nozzle temperature was set to 190 °C, the dimensions of printed products were more accurate. Ceretti et al. [16] found that support structure uniformity also affects dimensions, which could be optimized by adjusting the nozzle aperture and Z-axis height. Mohamed et al. [17] stated that layer thickness, air gap, raster angle, build orientation, road width, and a number of contours directly impact object dimensions. Moreover, they demonstrated the nonlinear relationship between printing parameters and dimensional accuracy through an I-optimality criterion and then used the desirability approach to obtain optimal printing parameters. In addition

to dimensional accuracy, the mechanical properties of printed objects also affect quality. Kuznetsov et al. [18] performed mechanical strength tests on printed objects with different nozzle sizes and layer thicknesses, and the results showed that a larger nozzle aperture can lead to an increase in the strength of a printed object under the same layer thickness. From the perspective of energy consumption in sustainable manufacturing, Khosravani et al. [12] and Simon et al. [19] found that most of the overall energy consumption is attributed to heating and maintaining the temperature of the nozzle/build plate. Hinshaw et al. [20] showed that the changes in layer thickness, printing speed, fan rate, and infill density also affect energy consumption. These studies point to a significant correlation between dimensional accuracy and energy consumption and show that both of them are affected by the same printing parameters.

The ultimate goal of sustainable manufacturing is to consider quality, environmental impact, cost, and even social issues together, causing a change in the optimization goal. Qattawi et al. [15] used the Taguchi method to study the relationship between the printing parameters and mechanical properties of printed objects, including dimensional accuracy, tensile strength, yield strength, and ductility. The results showed an inverse relationship between dimensional accuracy and mechanical strength. Thus, optimal parameters cannot directly yield the maximum mechanical strength and minimum dimensional tolerance. Khosravani et al. [12] indicated an inverse relationship between printing quality and energy consumption. To improve printing quality, more energy is consumed. Conversely, reducing energy usage results in poorer quality. Using the Taguchi method, D'Addona et al. [21] explored an optimization study of the cost and time of printing (by filament usage) and concluded that multiobjective optimization results vary with respect to different weights. Patil et al. [22] used grey relational analysis to study printing time and material usage and obtained optimized printing parameters. Moreover, Camposeco-Negrete [23,24] considered dimensional accuracy, mechanical strength, printing time, energy consumption, and material usage as optimization objectives and found that choosing a larger layer thickness helps in reducing printing time, energy consumption, and dimensional errors. Ransikarbum et al. [14] proposed a multiobjective optimization model that enables a batch of parts and multiple printers, and this model considers the operating cost, load balance among printers, total tardiness, and total unprinted parts.

Overall, based on a review of the previous literature, it can be concluded that changing printing parameters affects dimensional accuracy, energy consumption, and printing costs; moreover, simultaneously, there are a few contradictions with regard to the optimization of these three objectives. For example, a small layer thickness must be selected when it is required to decrease dimensional tolerance. However, this would increase energy consumption and material usage and, subsequently, the printing cost. In addition, the impact of energy consumption on the greenhouse effect must be more clearly quantified; the printing cost must consider the characteristics of different categories. In addition, under the consideration of different weights, multiobjective optimization parameters must be the same or different. In this study, five printing parameters that affect dimensional accuracy, carbon dioxide emissions, and three printing costs were selected, and several single-objective and multiobjective optimization tasks were implemented using the Taguchi method and desirability approach to generate sustainable manufacturing decisions.

The rest of this paper is organized as follows: Section 2 highlights the experimental design method and single-objective and multiobjective optimization methods, and Section 3 describes the results of single-objective optimization and multiobjective optimization. Section 4 discusses the relationship between printing parameters with regard to dimensional accuracy, carbon dioxide emissions, and the three printing costs. Finally, Section 5 summarizes the contribution and future work of this study.

2. Materials and Methods

2.1. Experimental Design

The five printing parameters affecting the dimensional accuracy, carbon dioxide emissions, and three printing costs are summarized by the literature review in Section 1, and they are the fan rate, printing speed, nozzle temperature, build plate temperature, and layer thickness. The printing parameter was considered due to the capability of the printing machine and the material properties of the filament. In addition, it is understood from experience that during the printing process using PLA material, the cooling fan must be turned on to avoid the situation of printing failure. Therefore, the fan rate is set to 50% and 100%. The range of the printing parameters is shown in Table 1. The 3D printer used in this study is the delta-type ATOM 2.5 EX [25], and the filament material is poly lactic acid (PLA) [26], which is environmentally friendly and easy to obtain. The printed object follows the ASTM-1708 standards [27], as shown in Figure 1. During the printing process, the object was placed at the center of the build plate without the need for any support materials. After printing, the outer width (OW), inner width (W), outer length (OL), and thickness (T) of every object were measured to determine the dimensional accuracy, as shown in Figure 2. The size was measured using Mahr's dial calipers [28], and an average of three values was used for recording.

Table 1. Printing parameters and ranges.

Factor	Printing Parameter	Range
A	Fan rate (%)	50~100
B	Print speed (mm/s)	20~30
C	Nozzle temperature (°C)	190~210
D	Build plate temperature (°C)	15~60
E	Layer thickness (mm)	0.1~0.3

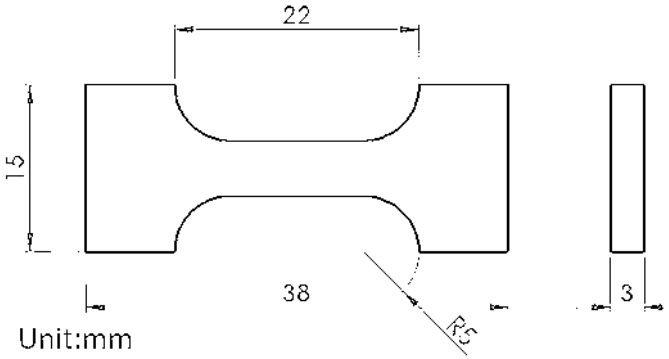

Figure 1. ASTM-D1708 specimen.

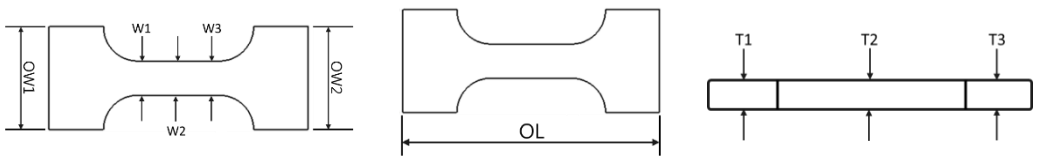

(**a**) Width (**b**) Length (**c**) Thickness

Figure 2. Standard measurement size.

The energy consumption of the printer during a printing cycle was recorded by a smart plug (TP-Link, HS100) [29]. The energy consumption data were updated every two seconds and then recorded in an Excel sheet. Therefore, the total energy consumption could be calculated from the time sequence. The printing cycle was divided into five stages,

as shown in Figure 3. Stage 1 involves heating the nozzle temperature to the set value and completing the incoming line procedure. Stage 2 aims at heating the build plate to the set temperature and maintaining the set temperature of the nozzle, and Stage 3 aims at printing the object. In Stage 4, the decline procedure is performed after printing, and the main step is heating the nozzle. In Stage 5, the filament is extracted, and the nozzle module returns to its original position. Carbon dioxide equivalent (CO_2e) is the standard unit for measuring CO_2 emissions. The concept is to use the same unit to express the degree of influence of different greenhouse gases (GHGs) on global warming. Thus, GHG sources with different CO_2 emissions could all be expressed using a single unit. The CO_2e of electricity production for Taiwan in the year 2021 was 0.502 kg CO_2e/degree. Therefore, the CO_2 emission during a printing cycle can be obtained using Equation (1).

$$\text{Carbon dioxide emission (kg } CO_2e/\text{degree)} = A \times 0.502 \quad (1)$$

where A is energy consumption (unit: kilowatt-hour).

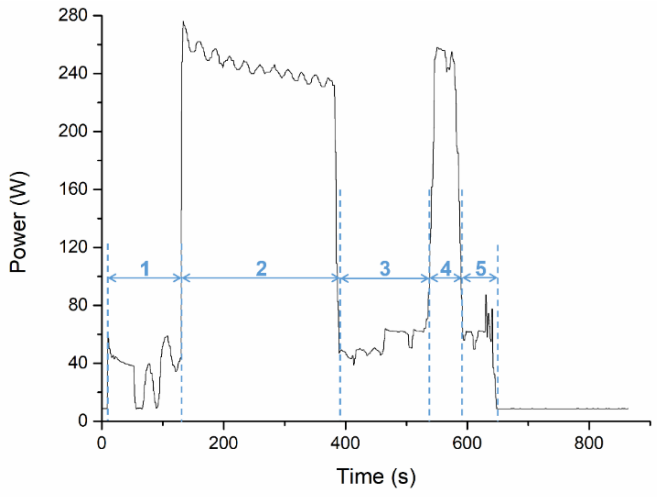

Figure 3. Energy consumption of printing cycle.

The three printing costs are related to electricity, filament, and labor. The electricity cost estimation is also based on the energy consumption of each printing operation recorded by the smart plug. The charging rate for industrial electricity for Taiwan in 2021 was TWD 2.6 per kilowatt-hour, and the electricity cost of each print is given by Equation (2).

$$\text{Electricity cost (\$NT)} = B \times 2.6 \quad (2)$$

where B is energy consumption (Unit: kWh).

The filament cost could be calculated using the usage amount and filament price. The total filament usage was obtained from the Cura software [30], and the price was TWD 2 per gram. The filament cost of each print could be calculated using Equation (3).

$$\text{Filament cost (\$NT)} = C \times 2 \quad (3)$$

where C is filament usage (unit: gram).

The labor cost is based on the printing time and statutory salary of the Taiwan government, which was calculated at TWD 168 per hour in 2021. In the printing process, staff only take some time to notice the situation, it is assumed 10% of occupation for every hour of printing. The labor cost of each print can be calculated using Equation (4).

$$\text{Labor cost (\$NT)} = D \times 16.8 \quad (4)$$

where D is printing time (unit: hour).

2.2. Methods for Single-Objective and Multiobjective Optimization

As requirements change, the dimensions of product manufacturing considerations change quantitatively. In this study, the product quality, carbon emissions, and cost that are emphasized in sustainable manufacturing are regarded as single-objective and multi-objective optimization goals. The single objectives are W, OW, OL, T, carbon dioxide emissions, material cost, labor cost, and electricity cost. The aim of the single-objective optimization in this study is to investigate the impact of the printing parameters on the FFF-3D printer using the Taguchi method. This method helps determine the significance and impact of different factors. The experimental matrix is referred to as an orthogonal array. The experiments were designed using the Taguchi method to help evaluate the impact of the five factors, namely the fan rate, print speed, nozzle temperature, build plate temperature, and layer thickness, on five important outputs, namely the dimensional accuracy, carbon dioxide emissions, electricity cost, material cost, and labor cost. Each factor consists of either two or three levels and was repeated three times to reduce the overall experimental errors (Table 2). To avoid the dependence of factors in the orthogonal array L18, we filled the factors only in lines 1, 3, 4, 5, and 6, as shown in Table 3.

Table 2. Level of each factor.

Factor	Printing Parameter	Degree of Freedom	Level 1	Level 2	Level 3
A	Fan rate (%)	2	100	50	-
B	Print speed (mm/s)	3	30	25	20
C	Nozzle temperature (°C)	3	210	200	190
D	Build plate temperature (°C)	3	60	30	15
E	Layer thickness (mm)	3	0.3	0.2	0.1

Table 3. Information of the 18 experiments.

Num.	1	3	4	5	6
	A	B	C	D	E
1	1	1	1	1	1
2	1	2	2	2	2
3	1	3	3	3	3
4	1	1	1	2	2
5	1	2	2	3	3
6	1	3	3	1	1
7	1	1	1	1	1
8	1	2	2	2	2
9	1	3	3	3	3
10	2	1	1	2	2
11	2	2	2	3	3
12	2	3	3	1	1
13	2	1	1	1	1
14	2	2	2	2	2
15	2	3	3	3	3
16	2	1	1	2	2
17	2	2	2	3	3
18	2	3	3	1	1

To choose appropriate factors and characterize their impacts, eight single-objective properties were investigated in terms of the signal-to-noise ratio (SNR). The SNR characteristics of these eight single objects (the lower the SNR, the better the performance characteristics) were calculated using Equations (5) and (6), and the SNR could be obtained

using the mean and standard deviations. The significance of the factors on all targets was then presented using the main effects plot. Finally, the contribution ratio of each factor could be obtained from the analysis of variance (ANOVA). ANOVA was used to interpret a series of experimental results to assess the significance of individual factors. The sum of squares and percentage contribution of each factor were denoted as SS_j and P_j, respectively, and their values could be obtained using Equations (6) and (7), respectively. In Equations (7) and (8), j is the individual parameter, and the total sum of squares is the SNR minus the correction factor.

$$S = \sqrt{\frac{\sum_{i=1}^{n}(y_i - \overline{y})^2}{n}} \tag{5}$$

$$\text{SNR} = -10 \cdot \log(\overline{y}^2 + S^2) \tag{6}$$

$$SS_j = \frac{1}{n_{P_j}} \sum_{j=1}^{k} \left(SNR_{P_j}\right)^2 - \frac{T^2}{n},\ T = \sum_{i=1}^{n} SNR_i \tag{7}$$

$$\rho_{P_j} = \left(\frac{SS_j}{SS_T}\right) \times 100\% \tag{8}$$

S: standard deviation of y;
y: observed data of the three single objectives;
$\overline{y}$: average of the observed data;
n: number of experiments.

Although the optimal printing parameters of the eight single objects can be obtained using the Taguchi method, it can be inferred that the optimal parameters of a single objective are different from the rest of the responses. A decision-making method that can simultaneously solve all the responses of the requirements must be incorporated to attain sustainable manufacturing. In this study, the desirability approach and different weights were used to obtain the optimal printing parameters under the simultaneous consideration of multiple objectives.

First, the implementation step aims at converting experimental values into expected values through the independent expectation function (individual desirability, D_i), as shown in Equation (9). Then, it aims at reconciling all independent expectation functions to obtain multiobjective optimal parameters through the composite expectation function (composite desirability, CD), as shown in Equation (10). Because all the goals in this study are characterized as "the smaller the better" and are equally significant, the weights were equally distributed to the evaluated goals. The closer the calculated value is to 1, the closer the process is to the ideal state. Conversely, the closer the value is to 0, the farther it is from the target.

$$D_i = \left[\frac{(U_i - y_i)}{(U_i - T_i)}\right]^{r_i} \tag{9}$$

D_i: desirability value of independence;
U_i: maximum value of the measurement;
y_i: measured value;
T_i: target value of the measurement;
r_i: weighting.

$$D_c = (D_1 \times D_2 \times D_3 \times \ldots D_n)^{\frac{1}{n}} \tag{10}$$

D_c: desirability value of the composite;
n: number of objective functions.

3. Results

3.1. Optimal Printing Parameters of All Single-Objective Optimizations

Figure 4 shows the parts after printing. Table 4 summarizes the mean values and S/N ratios of the experimental dimensional accuracy, carbon dioxide emissions, and three printing costs. Based on the results evaluated using Formula 6, the mean effects plot of each factor could be obtained, as shown in Figure 5, and the optimal parameters of all the single objectives could be calculated, as shown in Table 5. Finally, the factor contribution of each single objective could be obtained from the calculation of ANOVA, as shown in the Supplementary Material. Figure 6 summarizes the factor contributions of all the single objectives. From the perspective of dimensional accuracy optimization, when the width accuracy of the printed object is required, the values of the fan rate, printing speed, nozzle temperature, build plate temperature, and layer thickness should be set to 100%, 20 mm/s, 190 °C, 30 °C, and 0.3 mm, respectively. When the minimum tolerance of the thickness of a printed object is required, the optimal printing parameters should be changed to a fan rate of 50%, a printing speed of 20 mm/s, a nozzle temperature of 210 °C, a build plate temperature of 60 °C, and a layer thickness of 0.1 mm. However, if the carbon dioxide emissions and electricity cost are to be minimized, the fan rate, printing speed, nozzle temperature, build plate temperature, and layer thickness must be set to 100%, 30 mm/s, 190 °C, 15 °C, and 0.3 mm, respectively. The best printing parameters for reducing material costs were found to be a fan speed of 50%, a printing speed of 25 mm/s, a nozzle temperature of 200 °C, a build plate temperature of 30 °C or 15 °C, and a layer thickness of 0.3 mm. Finally, from the perspective of the lowest labor cost, the optimal printing parameters were found to be a fan speed of 50%, a printing speed of 30 mm/s, a nozzle temperature of 200 °C, a build plate temperature of 30 °C, and a layer thickness of 0.3 mm. The dimensional accuracy of W, material cost, and labor cost were most significantly affected by the layer thickness, and they were 52.81, 57.14, and 87.63%, respectively. Although delta-type machines are suitable for high-speed printing, errors in the rotation of the stepper motor, dimensions, pulley assembly, and toothed belt stretching affect the accuracy of printed parts [31]; in addition, the three-axis parallel motion link affects the end positioning due to kinematic errors, resulting in a larger error in the accuracy of printed parts with the increase in the distance from the center [32]. This caused the error to have the highest significance with regard to OW, OL, and T, which were 29.21, 29.73, and 45.12%, respectively. The CO_2 emissions and electricity cost were most significantly affected by the build plate temperature, with a contribution of 63.95%.

(**a**) top view (**b**) bottom view (**c**) side view

Figure 4. Parts after printing.

3.2. Optimal Printing Parameters of All Multiobjective Optimizations

To obtain a comprehensive decision-making approach to support sustainable manufacturing, in this study, we utilized the desirability approach analysis, which can help in obtaining the optimal printing parameters of the five multiobjective optimizations: multiobjective 1 (dimensional accuracy), multiobjective 2 (dimensional accuracy and carbon dioxide emissions), multiobjective 3 (three printing costs), multiobjective 4 (dimensional accuracy and three printing costs), and multiobjective 5 (dimensional accuracy and carbon dioxide emissions and three printing costs). Table 6 shows the optimal printing parameters of all the multiobjective optimizations with different weights. Multiobjective 1 is required

for all the needed dimensional accuracies (W, OW, OL, and T) of printed objects. Thus, each of the four dimensions has a weight of 25%. The optimal printing parameters calculated using the desirability analysis are as follows: a fan rate of 100%, a printing speed of 20 mm/s, a nozzle temperature of 210 °C, a build plate temperature of 60 °C, and a layer thickness of 0.1 mm.

Table 4. Mean values and S/N ratios of the experimental results.

Num.	W		OW		OL		T		Carbon Dioxide Emissions		Material Cost		Labor Cost		Electricity Cost	
	Mean	SNR	Mean	SNR	Mean	SNR	Mean	SNR	Mean	SNR	Mean	SNR	Mean	SNR	Mean	SNR
1	0.30	10.31	0.45	6.94	0.72	2.80	0.02	28.63	0.01	38.63	273.28	−48.73	2.43	−7.71	0.06	24.34
2	0.52	5.68	0.65	3.71	0.61	2.46	0.03	29.46	0.01	45.99	273.28	−48.73	4.28	−12.63	0.03	31.70
3	0.41	7.12	0.56	5.06	0.78	2.19	0.02	31.98	0.01	39.97	273.28	−48.73	10.48	−20.41	0.05	25.68
4	0.65	3.69	0.86	1.32	1.05	−0.42	0.06	24.20	0.01	45.99	273.28	−48.73	3.60	−11.13	0.03	31.70
5	0.67	3.42	0.65	3.65	0.87	1.21	0.03	29.46	0.01	41.55	273.28	−48.73	8.46	−18.55	0.04	27.26
6	0.32	9.75	0.49	6.23	0.71	2.98	0.03	30.02	0.01	39.97	273.28	−48.73	3.57	−11.04	0.05	25.68
7	0.59	4.00	0.69	2.57	0.85	1.04	0.05	24.50	0.03	32.01	273.28	−48.73	7.12	−17.05	0.13	17.72
8	0.31	10.18	0.53	5.54	0.70	3.08	0.13	17.79	0.00	46.28	266.88	−48.53	1.54	−3.76	0.03	31.99
9	0.47	6.55	0.63	3.97	0.87	1.24	0.03	29.21	0.01	43.49	273.28	−48.73	5.29	−14.48	0.03	29.20
10	0.68	3.27	0.75	2.55	0.95	0.48	0.09	20.92	0.01	45.99	273.28	−48.73	3.60	−11.13	0.03	31.70
11	0.59	4.65	0.66	3.57	0.86	1.31	0.01	36.99	0.03	32.01	273.28	−48.73	7.60	−17.62	0.13	17.72
12	0.38	8.03	0.56	4.90	0.78	2.03	0.06	22.42	0.00	46.59	266.88	−48.53	1.64	−4.31	0.02	32.30
13	0.55	5.24	0.93	0.54	1.43	-3.26	0.03	28.63	0.00	46.59	266.88	−48.53	1.47	−3.37	0.02	32.30
14	0.59	4.61	0.72	2.89	0.89	0.93	0.03	28.64	0.02	36.44	273.28	−48.73	4.28	−12.63	0.08	22.16
15	0.52	5.66	0.57	4.88	0.83	1.57	0.02	32.44	0.01	38.63	273.28	−48.73	8.32	−18.41	0.06	24.34
16	0.47	6.33	0.64	3.86	0.83	1.61	0.04	27.21	0.01	39.97	273.28	−48.73	7.12	−17.05	0.05	25.68
17	0.48	6.27	0.72	2.86	0.97	0.22	0.05	26.32	0.00	46.28	266.88	−48.53	1.54	−3.76	0.03	31.99
18	0.61	4.31	0.79	2.01	0.98	0.17	0.05	25.04	0.02	33.94	273.28	−48.73	5.29	−14.48	0.10	19.66

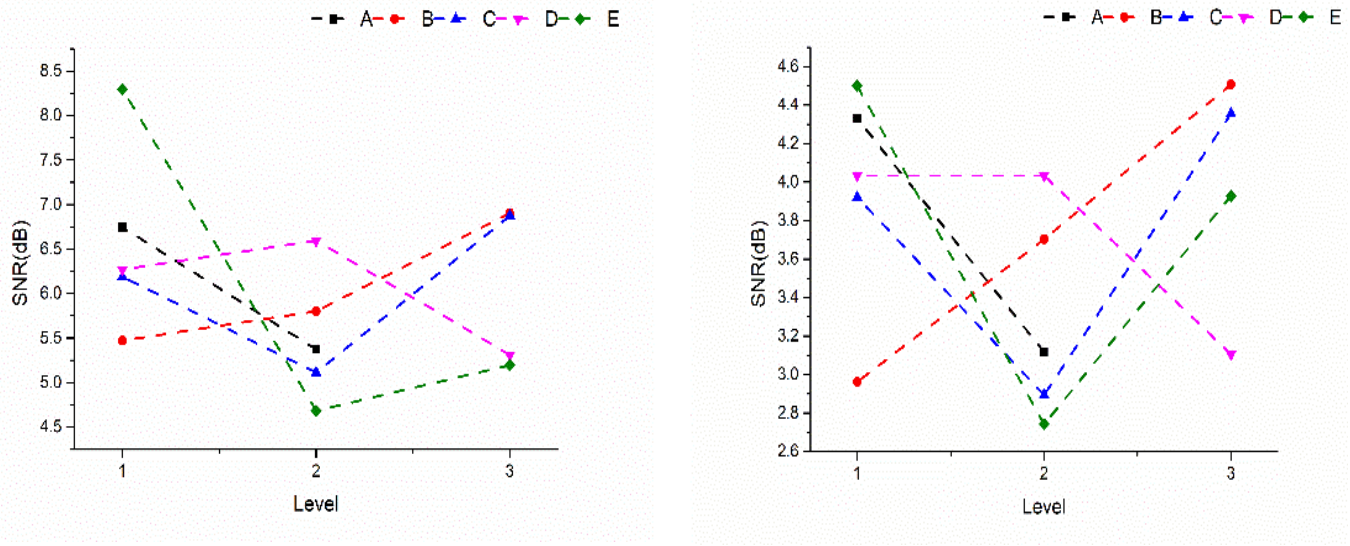

Figure 5. *Cont.*

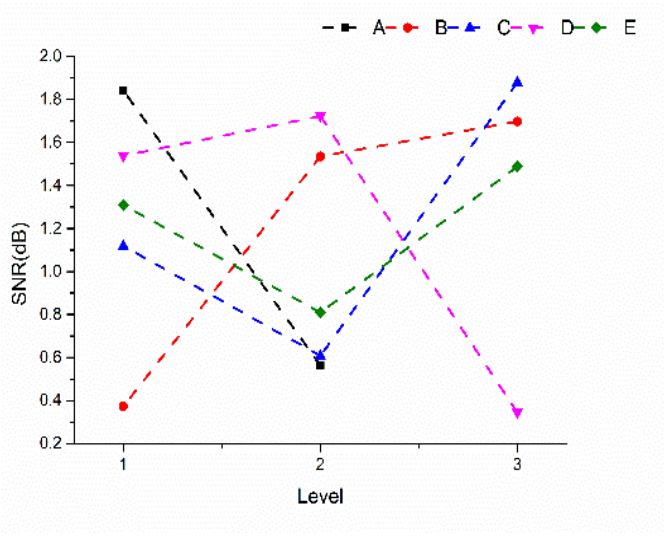

(**c**)

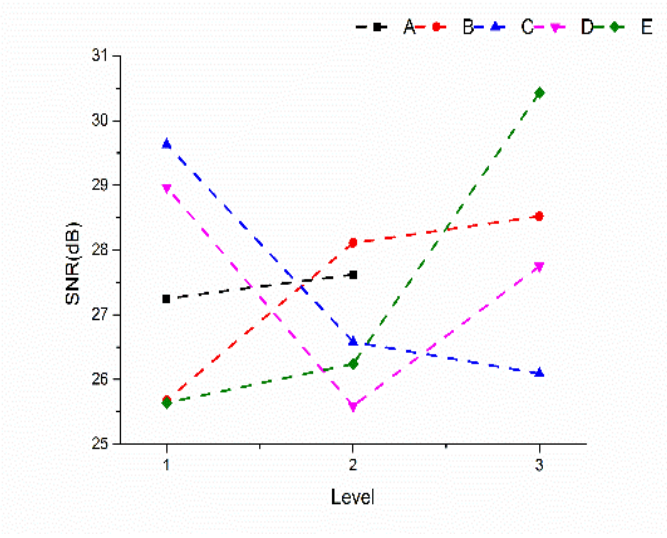

(**d**)

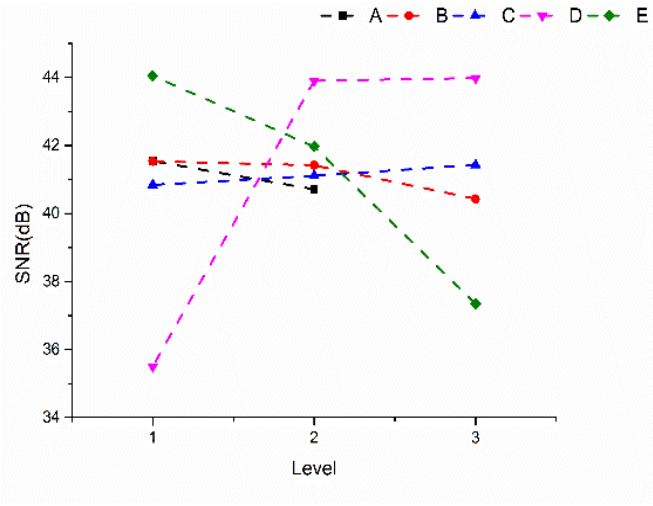

(**e**)

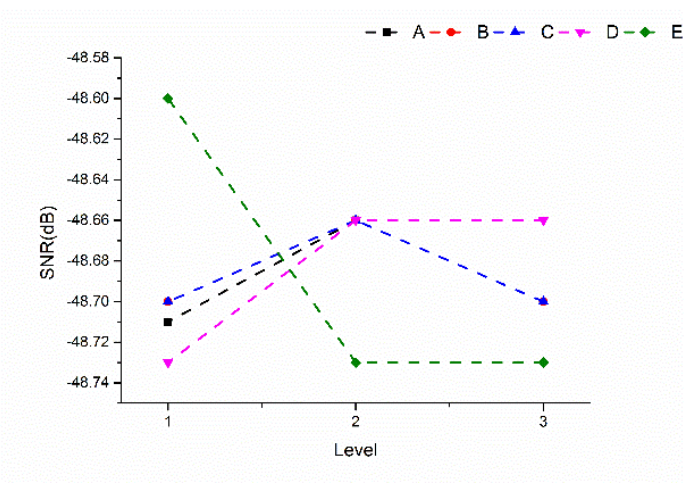

(**f**)

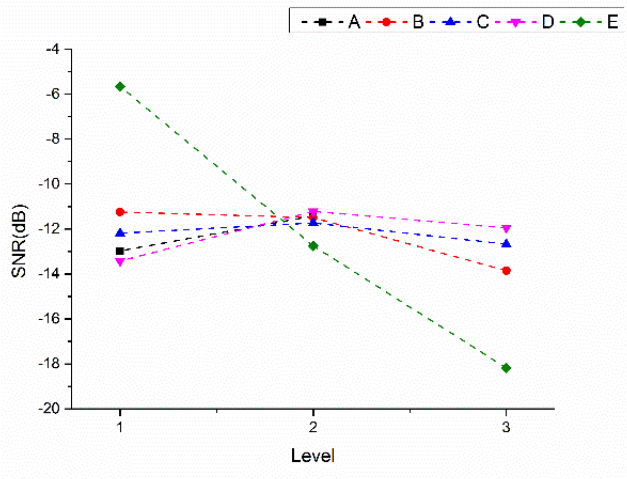

(**g**)

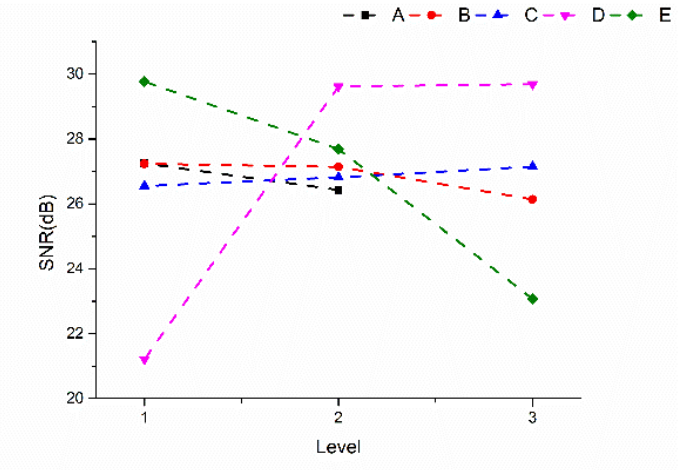

(**h**)

Figure 5. Mean effects plot: (**a**) W, (**b**) OW, (**c**) OL, (**d**) T, (**e**) carbon dioxide emissions, (**f**) material cost, (**g**) labor cost, (**h**) electricity cost.

Table 5. Optimal factors of all single objectives.

Optimization Object	Factor Importance	Optimal Factors
W	E > C > B > A > D	A1, B3, C3, D2, E1
OW	E > B > C > A > D	A1, B3, C3, D2, E1
OL	D > B > A > C > E	A1, B3, C3, D2, E3
T	E > C > D > B > A	A2, B3, C1, D1, E3
Carbon dioxide emission	D > E > B > A > C	A1, B1, C3, D3, E1
Material cost	E > D > A > B = C	A2, B2, C2, D2(3), E1
Labor cost	E > B > D > A > C	A2, B1, C2, D2, E1
Electricity cost	D > E > B > A > C	A1, B1, C3, D3, E1

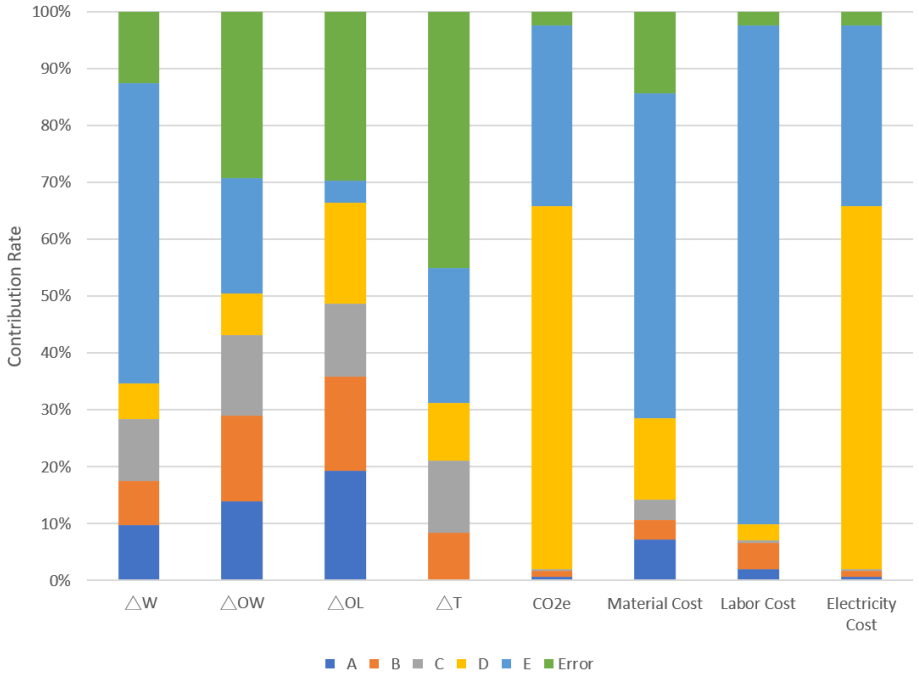

Figure 6. Factor contribution of all single objectives.

Table 6. All multiobjective optimal parameters.

Multiobjective	Optimization Object	Weight	Optimal Factors
1	Dimensional accuracy	Divide equally	A1, B3, C1, D1, E3
2	Dimensional accuracy and carbon dioxide emission	From 1:9 to 9:1	A1, B3, C1, D2, E2
3	3 printing costs	Divide equally	A2, B2, C2, D3, E1
4	Dimensional accuracy and 3 printing costs	From 1:9 to 9:1	A2, B3, C1, D1, E2
5	Dimensional accuracy, carbon dioxide emission, and 3 printing costs	Divide equally	A1, B3, C1, D2, E2
		8:1:1 4:2:4 2:2:6 1:1:8	A2, B3, C1, D2, E2
		Others	A1, B3, C1, D2, E2

The optimal printing parameters of multiobjective 2 under different weights are all the same, and they are as follows: a fan speed of 100%, a printing speed of 20 mm/s, a nozzle

temperature of 210 °C, a bottom plate temperature of 30 °C, and a layer thickness of 0.2 mm. The three printing costs in multiobjective 3 are equally weighted at 33.3%. The optimal printing parameters for multiobjective 3 are as follows: a fan speed of 50%, a printing speed of 25 mm/s, a nozzle temperature of 200 °C, a build plate temperature of 15 °C, and a layer thickness of 0.3 mm.

Multiobjective 4 is concerned with the dimensional accuracy and three printing costs. The optimal printing parameters under different weights are the same and are as follows: fan speed = 50%, printing speed = 20 mm/s, nozzle temperature = 210 °C, build plate temperature = 60 °C, and layer thickness = 0.2 mm. Multiobjective 5 is concerned with the dimensional accuracy, carbon dioxide emissions, and three printing costs. The optimal printing parameters are divided into three groups. The first group (equally weighted at 33.3%) is as follows: fan speed of 100%, a printing speed of 20 mm/s, a nozzle temperature of 210 °C, a bottom plate temperature of 30 °C, and a layer thickness of 0.2 mm. The optimal printing parameters of the second group (a weight of 8:1:1, 4:2:4, 2:2:6, and 1:1:8) are the same except for the fan speed of the optimal parameters in the first group, which was changed to 50%. Moreover, the optimal printing parameters of the third group (others) are the same as the optimal printing parameter in the first group.

4. Discussion

4.1. Printing Parameters in Different Single-Objective Optimizations

The variation of the five printing parameters under different single-objective optimizations can be explained through the following points: First, to achieve ideal results in W, OW, OL, carbon dioxide emissions, and electricity cost, the fan rate must be set to maximum (100%); however, the T, material cost, and labor cost should be reduced to 50%. Second, when the printing speed is set to 20 mm/s, W, OW, OL, and T show the best performance. However, to achieve the minimum carbon dioxide emissions, labor cost, and electricity cost, the printing speed should be increased to 30 mm/s. Simon et al. [19] and D'Addona et al. [21] highlighted that the printing speed affects the printing time, as the printing time is the accumulation of the nozzle movement. Therefore, reducing the printing time can also reduce carbon dioxide emissions. For the minimum material cost, the printing speed must be changed to 25 mm/s. Third, when the nozzle and build plate temperatures were set to 190 °C and 30 °C, respectively, the smallest dimensional errors in W, OW, and OL were obtained, which is consistent with the nozzle setting temperature suggested by Qattawi et al. [15]. However, to optimize T, it is necessary to increase the nozzle and build plate temperatures to 210 °C and 60 °C, respectively.

Regarding the carbon dioxide emissions and electricity cost due to energy consumption, Khosravani et al. [12] highlighted that the majority of the total energy consumption of an FFF-3D printer comes from heating and maintaining the nozzle and build plate temperatures. Since energy consumption is also positively related to electricity cost, setting the nozzle and build plate temperatures to 190 °C and 15 °C can help in obtaining minimal carbon dioxide emissions and electricity costs. Finally, a layer thickness of 0.1 mm can yield the best performance with regard to OL and T. Moreover, D'Addona et al. [21] mentioned that the layer thickness affects the number of layer thicknesses and amount of material used. Furthermore, Camposeco-Negrete [23] stated that a higher layer thickness can shorten the printing time, thus reducing the printing time and material usage and inevitably reducing the energy consumption and printing costs. As for the carbon dioxide emissions and three printing costs, using a layer thickness of 0.3 mm would be the best choice.

4.2. Printing Parameters in Different Multiobjective Optimizations

According to desirability analyses, the optimal printing parameters of multiobjective 1 and multiobjective 2 are different. If the minimum dimensional tolerance and carbon dioxide emissions are simultaneously required, it is necessary to increase the layer thickness and reduce the build plate temperature. For multiobjective 3, which only considers the minimum sum of the three printing costs, it is required to reduce the fan rate and the nozzle

and build plate temperatures, increase the printing speed, and choose the maximum layer thickness. The optimal parameters for multiobjective 4 can be seen as multiobjective 1 by reducing the fan rate and increasing the layer thickness. Although dimensional tolerances are slightly enlarged, lower fan rates and higher layer thicknesses do result in less energy and material consumption. Finally, it can be concluded that the optimal printing parameters for the majority of multiobjective 5 and multiobjective 2 are the same. This means that the lowest carbon dioxide emissions and three printing costs can be obtained while requiring the lowest dimensional tolerances. Simon et al. [19] mentioned that the heating area of the build plate is larger than that of the nozzle, which leads to higher energy consumption for heating and insulation. Therefore, choosing a lower build plate temperature can reduce electricity costs.

5. Conclusions

In this study, we identified the optimal printing parameters of the dimensional accuracy (W, OW, OL, and T), carbon dioxide emissions, and three printing costs in delta-type FFF-3D printers through several single-objective and multiobjective optimizations. The printing parameters are the fan rate, printing speed, nozzle temperature, build plate temperature, and layer thickness. The following conclusions could be drawn from this research:

1. The optimal parameters of single objectives were obtained using the S/N ratio and average effect plot. They are as follows: A1B3C3D2E1 in W; A1B3C3D2E1 in OW; A1B3C3D2E3 in OL; A2B3C1D1E3 in T; A1B1C3D3E1 in carbon dioxide emissions; A2B2C2D2(3)E1 in material cost; A2B1C2D2E1 in labor cost; and A1B1C3D3E1 in electricity cost. The optimal parameters of dimension W were the same as those of dimension OW, and only the layer thickness was different from dimension OL. Under the optimal parameters of dimension W, the difference could be improved by reducing the layer thickness. In addition, reducing the layer thickness and increasing the nozzle/build plate temperature must be implemented together to optimize dimension T. However, a higher temperature can result in higher carbon dioxide emissions and electricity costs, which can be eliminated by increasing the printing speed and lowering the build plate temperature.
2. The contribution and impact of each factor in different single-objective optimizations can be obtained using ANOVA. The dimensional accuracy of W, material cost, and labor cost are most significantly affected by the layer thickness. Although delta-type machines are suitable for high-speed printing, mechanism movement errors can affect the accuracy of printed parts, causing such errors to have the highest significance with regard to OW, OL, and T. The carbon dioxide emissions and electricity costs are most significantly affected by the build plate temperature.
3. Five objectives, namely the dimensional accuracy, carbon emissions, and three printing costs, could be optimized using a desirability analysis. In addition, through the desirability analysis and weights, different optimal printing parameters could be determined under the same multiple objectives. They are as follows: A1B3C1D1E3 in dimensional accuracy; A1B3C1D2E2 in dimensional accuracy and carbon dioxide emissions; A2B2C2D3E1 in three printing costs; A2B3C1D1E2 in dimensional accuracy and three printing costs; and A1(2)B3C1D2E2 in dimensional accuracy, carbon dioxide emissions, and three printing costs. The optimal printing parameters of the dimensional accuracy, carbon dioxide emissions, and three printing costs could be obtained in three different groups. This method is suitable for finding the optimal parameters with different weightings under multiple objectives. The optimal printing parameters for the dimensional accuracy and carbon dioxide emissions are the same as the majority for the dimensional accuracy, carbon dioxide emissions, and three printing costs. This means that the same set of printing parameters can be balanced across multiobjective optimizations, even if there are different weights in the objectives. Therefore, the best solution to achieve the full goal in terms of dimensional

accuracy is to only moderately reduce the build plate temperature and layer thickness values without minimizing them.

The surface roughness and mechanical properties are also important elements for evaluating printing quality. In future works, we aim to try to obtain optimized parameters of the surface roughness and tensile properties of printed objects through the S/N ratio and mean effects plot. In addition, we aim to add goals that affect environmental impacts so as to establish a more comprehensive relationship between printing quality and sustainable manufacturing.

Supplementary Materials: The following supporting information can be downloaded at: https://www.mdpi.com/article/10.3390/app121910060/s1, Table S1: Analysis of variance—△W; Table S2: Analysis of variance—△OW; Table S3: Analysis of variance—△OL; Table S4: Analysis of variance—△T; Table S5: Analysis of variance—CO_2e; Table S6: Analysis of variance—material cost; Table S7: Analysis of variance—labor cost; Table S8: Analysis of variance—electricity cost.

Author Contributions: Conceptualization, C.-J.Y.; methodology, C.-J.Y.; software, S.-S.W.; validation, C.-J.Y. and S.-S.W.; formal analysis, S.-S.W.; investigation, C.-J.Y.; resources, C.-J.Y.; data curation, C.-J.Y.; writing—original draft preparation, C.-J.Y. and S.-S.W.; writing—review and editing, C.-J.Y.; visualization, C.-J.Y.; supervision, C.-J.Y.; project administration, C.-J.Y.; funding acquisition, C.-J.Y. All authors have read and agreed to the published version of the manuscript.

Funding: The authors would like to thank the Ministry of Science and Technology, R.O.C., for financial support (MOST 111-2621-M-110-001 and MOST 110-2622-E-027-029).

Institutional Review Board Statement: Not applicable.

Informed Consent Statement: Not applicable.

Data Availability Statement: Not applicable.

Acknowledgments: Not applicable.

Conflicts of Interest: The authors declare no conflict of interest.

References

1. Calignano, F.; Manfredi, D.; Ambrosio, E.P.; Biamino, S.; Lombardi, M.; Atzeni, E.; Salmi, A.; Minetola, P.; Iuliano, L.; Fino, P. Overview on Additive Manufacturing Technologies. *Proc. IEEE* **2017**, *105*, 593–612. [CrossRef]
2. Boschetto, A.; Bottini, L. Design for manufacturing of surfaces to improve accuracy in Fused Deposition Modeling. *Robot. Comput. Manuf.* **2016**, *37*, 103–114. [CrossRef]
3. Valerga, A.P.; Batista, M.; Salguero, J.; Girot, F. Influence of PLA Filament Conditions on Characteristics of FDM Parts. *Materials* **2018**, *11*, 1322. [CrossRef] [PubMed]
4. Ottman, N.; Ruokolainen, L.; Suomalainen, A.; Sinkko, H.; Karisola, P.; Lehtimäki, J.; Lehto, M.; Hanski, I.; Alenius, H.; Fyhrquist, N. Soil exposure modifies the gut microbiota and supports immune tolerance in a mouse model. *J. Allergy Clin. Immunol.* **2018**, *143*, 1198–1206.e12. [CrossRef] [PubMed]
5. Conway, K.M.; Pataky, G.J. Crazing in additively manufactured acrylonitrile butadiene styrene. *Eng. Fract. Mech.* **2019**, *211*, 114–124. [CrossRef]
6. Heidari-Rarani, M.; Rafiee-Afarani, M.; Zahedi, A. Mechanical characterization of FDM 3D printing of continuous carbon fiber reinforced PLA composites. *Compos. Part B Eng.* **2019**, *175*, 107147. [CrossRef]
7. Ahmed, S.W.; Hussain, G.; Al-Ghamdi, K.A.; Altaf, K. Mechanical properties of an additive manufactured CF-PLA/ABS hybrid composite sheet. *J. Thermoplast. Compos. Mater.* **2019**, *34*, 1577–1596. [CrossRef]
8. Peng, A.; Xiao, X.; Yue, R. Process parameter optimization for fused deposition modeling using response surface methodology combined with fuzzy inference system. *Int. J. Adv. Manuf. Technol.* **2014**, *73*, 87–100. [CrossRef]
9. Gilmer, E.L.; Anderegg, D.; Gardner, J.M.; Sauti, G.; Siochi, E.J.; McKnight, S.H.; Dillard, D.A.; McIlroy, C.; Bortner, M.J. Temperature, diffusion, and stress modeling in filament extrusion additive manufacturing of polyetherimide: An examination of the influence of processing parameters and importance of modeling assumptions. *Addit. Manuf.* **2021**, *48*, 102412. [CrossRef]
10. Lunetto, V.; Priarone, P.C.; Galati, M.; Minetola, P. On the correlation between process parameters and specific energy consumption in fused deposition modelling. *J. Manuf. Process.* **2020**, *56*, 1039–1049. [CrossRef]
11. Byrley, P.; George, B.J.; Boyes, W.K.; Rogers, K. Particle emissions from fused deposition modeling 3D printers: Evaluation and meta-analysis. *Sci. Total Environ.* **2018**, *655*, 395–407. [CrossRef] [PubMed]
12. Khosravani, M.R.; Reinicke, T. On the environmental impacts of 3D printing technology. *Appl. Mater. Today* **2020**, *20*, 100689. [CrossRef]

13. Nyika, J.; Mwema, F.; Mahamood, R.; Akinlabi, E.; Jen, T. A five-year scientometric analysis of the environmental effects of 3D printing. *Adv. Mater. Process. Technol.* **2021**, 1–11. [CrossRef]
14. Ransikarbum, K.; Ha, S.; Ma, J.; Kim, N. Multi-objective optimization analysis for part-to-Printer assignment in a network of 3D fused deposition modeling. *J. Manuf. Syst.* **2017**, *43*, 35–46. [CrossRef]
15. Alafaghani, A.A.; Qattawi, A. Investigating the effect of fused deposition modeling processing parameters using Taguchi design of experiment method. *J. Manuf. Process.* **2018**, *36*, 164–174. [CrossRef]
16. Ceretti, E.; Ginestra, P.; Neto, P.; Fiorentino, A.; Da Silva, J. Multi-layered Scaffolds Production via Fused Deposition Modeling (FDM) Using an Open Source 3D Printer: Process Parameters Optimization for Dimensional Accuracy and Design Reproducibility. *Procedia CIRP* **2017**, *65*, 13–18. [CrossRef]
17. Mohamed, O.; Masood, S.; Bhowmik, J.L. Optimization of fused deposition modeling process parameters for dimensional accuracy using I-optimality criterion. *Measurement* **2016**, *81*, 174–196. [CrossRef]
18. Kuznetsov, V.E.; Solonin, A.N.; Urzhumtsev, O.D.; Schilling, R.; Tavitov, A.G. Strength of PLA Components Fabricated with Fused Deposition Technology Using a Desktop 3D Printer as a Function of Geometrical Parameters of the Process. *Polymers* **2018**, *10*, 313. [CrossRef]
19. Simon, T.R.; Lee, W.J.; Spurgeon, B.E.; Boor, B.E.; Zhao, F. An Experimental Study on the Energy Consumption and Emission Profile of Fused Deposition Modeling Process. *Procedia Manuf.* **2018**, *26*, 920–928. [CrossRef]
20. Hinshaw, H.J.; Terry, S.; Fidan, I. Power consumption investigation for fused filament fabricated specimen. *Int. J. Rapid Manuf.* **2020**, *9*, 268. [CrossRef]
21. D'Addona, D.; Raykar, S.J.; Singh, D.; Kramar, D. Multi Objective Optimization of Fused Deposition Modeling Process Parameters with Desirability Function. *Procedia CIRP* **2021**, *99*, 707–710. [CrossRef]
22. Patil, P.; Singh, D.; Raykar, S.J.; Bhamu, J. Multi-objective optimization of process parameters of Fused Deposition Modeling (FDM) for printing Polylactic Acid (PLA) polymer components. *Mater. Today Proc.* **2021**, *45*, 4880–4885. [CrossRef]
23. Camposeco-Negrete, C. Optimization of printing parameters in fused deposition modeling for improving part quality and process sustainability. *Int. J. Adv. Manuf. Technol.* **2020**, *108*, 2131–2147. [CrossRef]
24. Camposeco-Negrete, C. Optimization of FDM parameters for improving part quality, productivity and sustainability of the process using Taguchi methodology and desirability approach. *Prog. Addit. Manuf.* **2020**, *5*, 59–65. [CrossRef]
25. ATOM. 3D Delta Printer. Available online: https://www.atom3dp.com/ (accessed on 31 March 2022).
26. FEASUN. Basic Type of PLA. Available online: https://www.feasun3d.com/product/min-yau-pla1/ (accessed on 31 March 2022).
27. ASTM Standard D1708. Standard Test Method for Tensile Testing of Plastics Using Microtensile Specimens. Available online: https://www.intertek.com/polymers/tensile-testing/astm-d1708/ (accessed on 31 March 2022).
28. Mahr. Dialcalipers. Available online: https://www.mahr.com/de/ (accessed on 31 March 2022).
29. TP-Link. Smart Plug. Available online: https://www.tp-link.com/tw/ (accessed on 31 March 2022).
30. ATOM Cura. Slicer. Available online: https://reurl.cc/nO35Xn (accessed on 31 March 2022).
31. Incekar, E.; Kaygisiz, H.; Babur, S. Dimensional Accuracy Analysis of Samples Printed in Delta and Cartesian Kinematic Three Dimensional Printers. *J. Polytech.* **2020**, *24*, 529–537. [CrossRef]
32. Kochetkov, A.V.; Ivanova, T.; Seliverstova, L.V.; Zakharov, O.V. Kinematic Error Modeling of Delta 3D Printer. *Mater. Sci. Forum* **2021**, *1037*, 77–83. [CrossRef]